COMMUNICATIONS TO THE EDITOR

Laminar Boundary Layers on Continuous Flat and Cylindrical Surfaces

E. A. KOLDENHOF
Central Research Institute of A.K.U., Arnhem, Holland

For some years we have studied, both theoretically and experimentally, the group of boundary-layer problems which play a part in the manufacture of rayon and fully synthetic threads and films. These problems have recently been described by Sakiadis (*1*, *2*, *3*). With respect to the laminar boundary layer on a continuous cylinder the following may be remarked.

The boundary-layer equation, written in cylindrical coordinates (*4*), is

$$ru\frac{\partial u}{\partial x} + rv\frac{\partial u}{\partial r} = \nu\frac{\partial}{\partial r}\left(r\frac{\partial u}{\partial r}\right) \quad (1)$$

and the equation of continuity becomes

$$\frac{\partial}{\partial r}(rv) + r\frac{\partial u}{\partial x} = 0 \quad (2)$$

The boundary conditions on the wall of the cylinder are

$$r = a\colon \frac{\partial^2 u}{\partial r^2} + \frac{1}{a}\frac{\partial u}{\partial r} = 0;\ u = v_o$$

If we use dimensionless variables $V \propto = \dfrac{u}{v_o}$, $\zeta = \dfrac{r-a}{a}$ these boundary conditions become

$$\zeta = 0\colon \frac{\partial^2\alpha}{\partial\zeta^2} + \frac{\partial\alpha}{\partial\zeta} = 0;\ \alpha = 1 \quad (3)$$

With the analogy of the so-called *Pohlhausen solution* of Glauert and Lighthill for the finite cylinder, a solution for the continuous cylinder can be obtained. We differentiate the boundary-layer equation; when the equation of continuity and dimensionless variables are used, we obtain for $\zeta = 0$

$$\frac{\partial^3\alpha}{\partial\zeta^3} + \frac{\partial^2\alpha}{\partial\zeta^2} - \frac{\partial\alpha}{\partial\zeta} = 0 \quad (4)$$

This equation can be solved by forming a power series

$$\alpha = \frac{1}{B}\sum_{n=0}^{\infty}\frac{C_n}{n!}\zeta^n \quad (5)$$

The first three constants can be obtained from the boundary conditions on the wall of the cylinder and from Equation (3). We get

$$C_0 = B,\ C_1 = -1,\ C_2 = 1$$

The other coefficients can be obtained

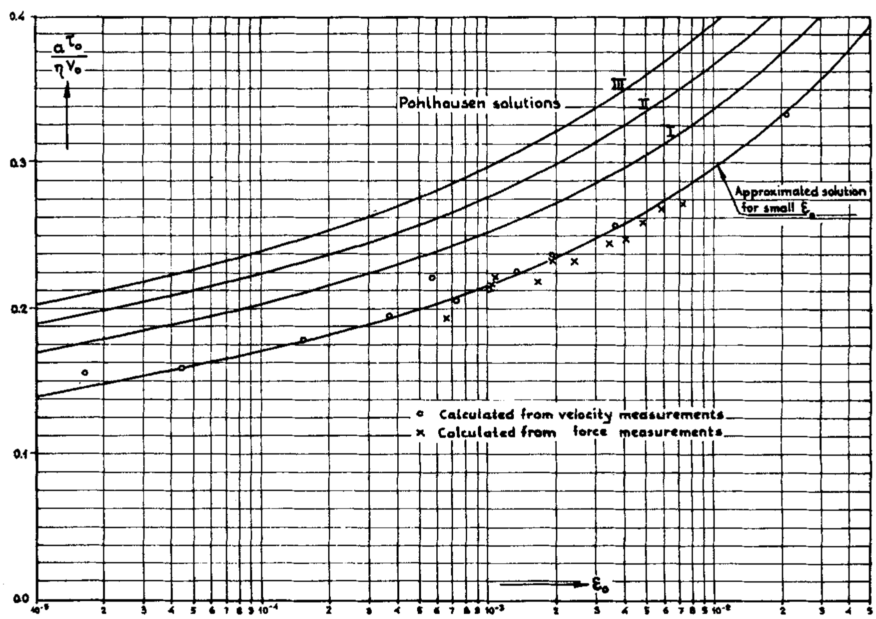

Fig. 1. Theoretical and experimental data for the description of the boundary layer on the continuous cylinder.

Abstracts and Key Words

Of the latest book in the Chemical Engineering Progress Symposium Series

HEAT TRANSFER—HOUSTON

Vol. 59, No. 41, 1963, $3.50 to members, $15.00 to nonmembers. Symposium Series books may be ordered from the Secretary's Office, the American Institute of Chemical Engineers, 345 East 47 Street, New York 17, New York.

Key Words: Computer-10, Regression Analysis-10, Heat Transfer-2, 7, 8, Air Cooling-2, Pressure Drop-7, 8, Transferring-2, 7, 8, Finned Tubes-10, Geometry-6, Pitch-6, Nusselt-7, F-Level-10, Friction Factor-8, Correlation-8, Helical Fin-6, Fin Thickness-6, Fin Height-6, Fin Spacing-6, Convection-10, Tube Bank-10, Heat Exchangers-10, Velocity-6, Reynolds Number-6, Air-5, 9.

Abstract: The previous investigation reported by Ward and Young (1) on the effects of tube geometry on the heat transfer and pressure drop characteristics of equilateral-triangular-pitch tube banks containing smooth, integral, helically, finned tubes with air drawn by forced convection in cross flow through seven finned tube banks was extended to cover nine additional banks of tubes. Data were taken to determine the effect of fin thickness and tube pitch on the air film heat transfer coefficient. Improved heat transfer correlations are presented. Air side pressure drop data are reported which include the effects of tube pitch.

Reference: Briggs, Dale E., and Edwin H. Young, Chem. Eng. Progr. Symposium Ser. No. 41, 59, p. 1 (1963).

Key Words: Heat Transfer-8, Fluid Flow-8, Flow Distribution-8, Heat Exchanger-10, Cross Flow Exchangers-10, Analogue Study-, Fluids-1, Tube Bank-10, Manifolds-10, Heat Exchanger Performance-8.

Abstract: To evaluate the effects of nonuniform distribution of tube side flow on the total heat transfer in single pass, cross flow exchangers, an investigation was carried out with electronic analogue equipment. Results of runs for which the operating values were equal, but for which flow distributions were different, were compared and the influence of various operating parameters was studied. It was found that for a given set of operating conditions, the maximum deviation of total heat transfer with nonuniform tube flow characteristics from that obtained under uniform flow conditions was ~4%.

Reference: McDonald, J. S., and K. Y. Eng, Chem. Eng. Progr. Symposium Ser. No. 41, 59, p. 11 (1963).

Key Words: Thermoelectric Generator-8, Heat-1, Electric Power-2, Cooling Device-4, Natural Convection-4, Transverse-Fins-4, Heat Transfer-4, Air-5, Velocity-6, Pressure Drop-6, Pumping Power-6, Temperature Differential-6, Power Output-7, Heat Transfer-8, Cooling-8, Thermoelectric Elements-9, Heat Transfer-10, Experiments-10, Convective-.

Abstract: Two types of cooling devices for a thermoelectric generator are described, and performance data are reported. The first one, a wire-coiled extended surface, removes heat through the natural convection mode; the second one, a transverse-finned surface, makes use of forced convection heat transfer for relatively large power output units.

Reference: Gritton, D. G., and Y. S. Tang, Chem. Eng. Progr. Symposium Ser. No. 41, 59, p. 18 (1963).

(Continued on page 413)

* For details on the use of these key words and the A.I.Ch.E. Information Retrieval Program, see Chem. Eng. Progr., 57, No. 5, p. 55 (May, 1961), No. 6, p. 73 (June, 1961); 58, No. 7, p. 9 (July, 1962).

by differentiating Equation (4). In this way we find for Equation (5)

$$\alpha = 1 - \frac{1}{B}\left\{\zeta - \frac{\zeta^2}{2} + \frac{\zeta^3}{3} - \frac{\zeta^4}{8} + \frac{\zeta^5}{24} \ldots\right\} \quad (6)$$

At this point it should be remarked that Equation (6) is very similar to the equation of Glauert and Lighthill; there is only a difference in the value of C_0 which is zero for the finite cylinder.

If $\zeta < 1$, then Equation (6) may also be written

$$\alpha = 1 - \frac{1}{B}\ln(1+\zeta) \quad (7)$$

The deviation of (7) with respect to (6) is of the order of magnitude of $o(\zeta^4)$. The thickness of the boundary layer, δ, now follows from (2)

$$\delta = a\,(e^B - 1) \quad (8)$$

The constant B is a function of the distance to the commencement of the boundary layer x and can be determined by using the momentum equation. It appears that B may be written as a function of the dimensionless quantity

$$\epsilon_0 = \frac{v_0 a^2}{2\nu x} \quad (9)$$

From the momentum equation we find that B must be calculated from the following relation

$$\frac{1}{B}(e^{2B} - 1) - 2 - \sum_{m=1}^{\infty} \frac{(2B)^m}{m.\,m!} = \frac{1}{\epsilon_0} \quad (10)$$

The series in (10) can be found in a simple manner by using the tabulated solution of the exponential integral, for example, Jahnke, Emde, and Lösch, (5), where

$$\sum_{m=1}^{\infty} \frac{(2B)^m}{m.\,m!} = \overline{E_L}\,(2B) - \ln 2B - 0.5772$$

The solution given by (7) and (10) is in complete agreement with that derived by Sakiadis. Equation (10) can be obtained from the Sakiadis solution by analytical integration. In the case of flows around textile threads we are mostly concerned with a small value of a (or ϵ_0). In this case an approximate solution can be derived from (12)

$$\frac{1}{2B}e^{2B} = \frac{1}{\epsilon_0} \quad (11)$$

If $a \to 0$ (or $\epsilon_0 \to 0$) it follows from (10) that $B \to \infty$ and, consequently, from (8) that $\delta \to \infty$. For small values of a the condition that $\zeta < 1$ is therefore only fulfilled in a relatively thin part of the boundary layer adjacent to the surface of the cylinder. The deviation between the solutions (6) and (7) will therefore become greater when $a \to 0$.

The question now is, which of these two solutions will give the best results in describing the boundary layer for small values of a. On the one hand, solution (6) is derived from the boundary-layer equation and the equation of continuity on the wall of the cylinder; on the other hand, in the case of solution (7) the deviation from the boundary conditions on the outside of the boundary layer tends to zero [see Sakiadis (3)].

A more theoretical answer to this question can be given in the following way. We introduce as new variables

$$\alpha = \frac{u}{v_o}, \beta = \frac{x\,v}{a\,v_o}. \gamma = \ln\frac{r}{a}\ \xi = \frac{rx}{a^2}$$

Equation (1) then reads

$$\frac{\partial^2\alpha}{\partial\gamma^2} = -2\epsilon_0\,\alpha^2\frac{\partial}{\partial\gamma}\left(e^{\gamma}\frac{\beta}{\alpha}\right) \quad (12)$$

and Equation (2)

$$e^{2\gamma}\frac{\partial\alpha}{\partial\xi} + \frac{\partial}{\partial\gamma}(e^{\gamma}\beta) = 0$$

with the appropriate boundary conditions

$$\gamma = 0: \quad \alpha = 1, \quad \beta = 0;$$
$$\gamma = \infty: \quad \alpha = 0.$$

From (12) it follows that if $\epsilon_0 \to 0$ and if, for $\gamma = \gamma^1$, the quantity $\frac{\partial}{\partial\gamma}\left(e^{\gamma}\frac{\beta}{\alpha}\right)$ remains finite, the first equation of (12) at γ_1, can be approximated with increasing accuracy by

$$\frac{\partial^2\alpha}{\partial\gamma^2} = 0 \quad (13)$$

The solution of (13) is the above-mentioned Equation (7), and, consequently, also Equation (10).

We already mentioned that $\delta \to \infty$ if $\epsilon_0 \to 0$. This results in a decrease of the error incurred when in the momentum equation δ instead of ∞ is taken as boundary condition. Therefore, in the extreme case of $\epsilon_0 = 0$ (7) represents the exact solution for the boundary-layer equation. From (12), and with the aid of (10), we can estimate the magnitude of the deviation from

(*Continued from page 412*)

INFORMATION RETRIEVAL

Key Words: Conduction of Heat-1, Gun Barrel Cooling-2, Gun Barrel Heating-3, Gun Cooling-4, Gun Heating-5, Heat Conduction-6, Heat Transfer-7, Periodic Heat Source-8, Transient Heat Conduction-9, Unsteady State Heat Conduction-10.

Abstract: A cannon is fired in a series of bursts while being cooled externally. The maximum bore surface temperature and the maximum value of the space average temperature are calculated. Results are presented in a form useful to a gun designer.

Reference: Fagan, Walter, **Chem. Eng. Progr. Symposium Ser. No. 41, 59,** p. 25 (1963).

Key Words: A. Heat Transfer-7, 8, 9, Pressure Drop-7, 8, 9, Heat Transfer Coefficient-7, 8, Friction Factor-7, 8, Drag Coefficient-7, 8, Turbulence Promoter-6, 8, 10, Water-9, 10, Disk-9, 10, Streamline Shape-9, 10, Axial Core-9, 10, Annulus-9, 10, Correlation-8, Heat Exchanger-9, 10, Rate-7, 8, Nusselt Number-7, 8, Reynolds Number 6, 8, Geometry-6, 8, Tubes-9, 10, Performance-8, Transfer-Ring-6, 7, 8, 9, Improving-6, 7, 8, 9, Bluff-Body-9, 10, Size-6, 8, Spacing-6, 8.

Abstract: The pressure drop and rate of heat transfer were measured for water flowing in a tube containing bluff-body promoters. Disks and streamline shapes of several sizes were mounted at various uniform spacings along a small, axially centered rod. Solid axial cores of various uniform diameters were also investigated. General empirical correlations are presented for the heat transfer coefficient and effective drag coefficient or friction factor for disks, streamline shapes, and annuli.

Reference: Evans, Larry B., and Stuart W. Churchill, **Chem. Eng. Progr. Symposium Ser. No. 41, 59, p.** 36 (1963).

Key Words: Tube-8, Inlet Region-6, Heat Exchanger-10, Air-5, Temperature-6, Nusselt Number-8, Calorimeter-10, Thermocouples-10, Burner-10.

Abstract: Local film heat transfer coefficients for a gas flowing in the entrance region of a circular tube were experimentally determined for temperatures up to 1,112°F. and a Reynolds number of 19,623. A novel method based on measuring steam produced in insulated compartments which surrounded the tube and contained saturated water was used to determine the coefficients. Results for a sharp edged entrance were compared with previous investigators and a correlation was presented for the entrance region.

Reference: Davey, T. B., **Chem. Eng. Progr. Symposium Ser. No. 41, 59,** p. 47 (1963).

Key Words: Liquid-1, Boiling-1, Nucleation-1, Phase Change-1, Active Sites-1, Vapor-2, Bubbles-2, Vapor Column-2, Statistics-6, Site Distribution-6, Mechanism-6, Boiling Properties-7, Thermodynamic-7, Hydrodynamic-7, Heat Transfer-8, Nucleate Boiling-8.

Abstract: Statistical analysis of existing data shows that the local population densities of active boiling nucleation sites fit a Poisson distribution. Expressions are obtained for the distribution of nearest-neighbor distances and the average distances between nucleation sites. From this result means are available for relating the nucleation properties of the surface with local hydrodynamic and thermodynamic processes in a quantitative analysis of nucleate boiling.

It is concluded that patch-by-patch boiling is only a visual manifestation of a completely random spatial distribution of nucleation sites, and that the dependence of site population on surface temperature is in accordance with nucleation theory.

Reference: Gaertner, R. F., **Chem. Eng. Progr. Symposium Ser. No. 41, 59,** p. 52 (1963).

(*Continued on page 414*)

(*Continued from page 413*)

INFORMATION RETRIEVAL

Key Words: Boiling, subcooled-8, Subcooled boiling-8, Mixtures-6, Alcohols-10, Burnout-8, Burnout flux-8.

Abstract: Binary aqueous mixtures of lower alcohols and the pure components were subjected to subcooled nucleate boiling in an annulus on the surface of an electrically heated 1/4-in. O. D. stainless steel inner tube. Data were obtained at a pressure of 30 lb./sq. in. abs. and a velocity of 4 ft./sec. with subcooling between 60° and 110°F.

The data indicate that greater superheat is required to produce a given heat flux for the mixtures than for either of the pure components. For each mixture the maximum superheat occurs at composition predominant in high boiler. Burnout data were obtained for some compositions.

Reference: Rose, William H., Herbert L. Gilles, and Vincent Uhl, **Chem. Eng. Progr. Symposium Ser. No. 41, 59,** p. 62 (1963).

Key Words: Heat Exchange-7, Heating-10, Boiling-8, Vaporization-8, Burnout-8, Axial Flow-13, Swirl Flow-13, Cross Flow-13, Properties-6, Organic Fluid-9, Hydrazine-9, Ammonia-9, Diphenyl-9, Nitrogen Tetroxide-9, Ethylene Glycol-9, Monoisopropylbiphenyl-9, Water-9.

Abstract: A generalized two-term additive prediction method has been developed in which one term represents the boiling contribution to the burnout heat flux in the absence of forced convection and the other the equivalent forced-convection contribution in the absence of boiling. The predictions of this superposition method have been compared with all available experimental data (1,326 points) for burnout with flowing, wetting liquids in the absence of significant net vapor generation. The data compared are for seven fluids in axial, swirl, and cross flow in tubular, annular, rectangular, and rod geometries over very broad ranges of flow conditions.

Reference: Gambill, W. R., **Chem. Eng. Progr. Symposium Ser. No. 41, 59,** p. 71 (1963).

Key Words: Boiling-1, 2, 8, Pressure Transients-4, 5, 6, 8, Burnout-2, 7, 8, Pool Boiling-1, 2, 8, Transient-5, 8, Heat Transfer-1, 2, 8, Temperature Transients-5, 7, 8, Predicting-8, Nucleation-1, 8, Stainless Steel-5, 8, Horizontal Strips-5, 8, Stainless Steel-Water-5, 8, Nucleate Boiling-1, 2, 8, Saturation-1, 2, 8.

Abstract: The effect of pressure decay on burnout in pool boiling of water is investigated. Initial saturation conditions were allowed to decay to 1 atm., and the time to burnout of a stainless steel ribbon with constant internal heat generation was studied. Results are correlated on the basis of the pressure vs. burnout heat flux curve for steady state pressure for the system. Time to burnout was longer than predicted from the steady state curve and decay rate.

Reference: Howell, J. R., and K. J. Bell, **Chem. Eng. Progr. Symposium Ser. No. 41, 59,** p. 88 (1963).

Key Words: Flow Oscillations-8, Unstable-8, Dynamical Behavior-8, Heat Transfer Loop-9, Two-phase Flow-9, Natural Convection-9, Natural Circulation Loop-9, Boiling-9, Two-phase Pressure Drop-9, Steam Volume Fraction-9, Vapor-liquid Velocity Ratio-9, Conservation Equations-10, Analogue Computer-10.

Abstract: The time and space dependent conservation equations are applied to a natural circulation boiling water loop. The equation set is solved on an analogue computer, and the results are compared with experimental loop results. The comparison shows the analogue model capable of predicting steady state loop behavior, loop behavior with sinusoidally power input and power level at which the loop oscillates.

Reference: Anderson, R. P., L. T. Bryant, J. C. Carter, and J. F. Marchaterre, **Chem. Eng. Progr. Symposium Ser. No. 41, 59,** p. 96 (1963).

(*Continued on page 415*)

the ln-velocity profile at small values of ϵ_0. For this purpose α is written in a Taylor series. Taking into account that $\alpha = 1$ and $\frac{\partial^2\alpha}{\partial\gamma^2} = 0$ at $\gamma = 0$ this series reads as follows

$$\alpha = 1 - \frac{\gamma}{B} + \frac{1}{3!}\left(\frac{\partial^3\alpha}{\partial\gamma^3}\right)_{\gamma=0}\gamma^3 + \frac{1}{4!}\left(\frac{\partial^4\alpha}{\partial\gamma^4}\right)_{\gamma=0}\gamma^4 + \qquad (14)$$

The third and higher derivatives of α with respect to γ are calculated from (12).

To this end the boundary-layer equation can be written

$$\frac{\partial^2\alpha}{\partial\gamma^2} = 2\epsilon_0\left(\alpha\, e^{2\gamma}\frac{\partial\alpha}{\partial\xi} + \beta\, e^{\gamma}\frac{\partial\alpha}{\partial\gamma}\right) \qquad (15)$$

For $\frac{\partial\alpha}{\partial\xi}$ at small values of ϵ_0, we find from the approximated solution given by (7) and (10)

$$\frac{\partial\alpha}{\partial\xi} = \frac{\partial\alpha}{\partial B}\times\frac{\partial B}{\partial x}\times\frac{\partial x}{\partial\xi} = \frac{2}{R_{ea}}\,\frac{e^{-2B}}{B-1}\,\gamma e^{-\gamma}$$

so that (15) can also be written

$$\frac{\partial^2\alpha}{\partial\gamma^2} = \frac{\partial\alpha}{x}\,\frac{e^{-2B}}{B-1}\,\alpha\,\gamma\, e^{\gamma} + 2\epsilon_0\,\beta e^{\gamma}\frac{\partial\alpha}{\partial\gamma}$$

Differentiating this formula a few times with respect to γ and each time putting $\gamma = 0$, we find for (14)

$$\alpha = 1 - \frac{\gamma}{B} + \frac{1}{K}\left\{\frac{1}{6}\gamma^3 + \frac{1}{24}\left(2 - \frac{1}{B}\right)\gamma^4 + \frac{1}{120}\left(3 - \frac{4}{B} - \frac{2}{K}\right)\gamma^5 + \ldots\right\} \qquad (16)$$

where

$$\frac{1}{K} = \frac{2a}{x}\,\frac{e^{-2B}}{B-1}$$

Using Equation (10) the latter formula can also be written

$$\frac{1}{K} = \frac{2a}{x}\,\epsilon_0\,\frac{1}{2B(B-1)}$$

For a small value of ϵ_0 and, consequently, a large value of B and k Equation (16) may also be written

$$\alpha = 1 - \frac{\gamma}{B} + \frac{1}{K}\sum_{n=3}^{\infty}\frac{n-2}{n}\gamma^n$$

TABLE 1. DIFFERENCE: $\alpha(17) - \alpha(7)$ AS A FUNCTION OF γ AT $B = 3.4$ (THAT IS, $\epsilon_0 \approx 10^{-2}$) AND $\frac{2a}{x} = 10^{-2}$

γ	$\Delta\alpha$
0	0
0, 5	1, 62 10^{-7}
1, 0	1, 73 10^{-6}
1, 5	7, 72 10^{-6}
2, 0	2, 45 10^{-5}
2, 5	9, 00 10^{-5}
3, 0	1, 54 10^{-4}
3, 4	2, 90 10^{-4}

Note: $\gamma\delta = \ln \frac{\delta + a}{a}$ now is 3.401 instead of 3.400.

or

$$\alpha = 1 - \frac{\gamma}{B} + \frac{1}{K}(\gamma e^{\gamma} - 2e^{\gamma} + \gamma + 2) \tag{17}$$

Since $\frac{1}{K}$ not only depends on B and ϵ_0, but also on $\frac{a}{x}$, α now also is a function of $\frac{a}{n}$

Apparently this dependence, which is also to be expected from the boundary-layer equation, is only of secondary importance for a small value of ϵ_0. By way of example we have given in Table 1 the difference between the velocity calculated from (7) and that calculated from (17) for different values of γ. This example has been so chosen that for most of the boundary layers occurring in practice the deviations from (7) are even smaller.

Not only for small, but also for large values of ϵ_0, the accuracy with which, for instance, (10) describes the actual flow calls for some comment. For $a \to \infty$ ($\epsilon_0 \to \infty$) the flow around a cylinder will change to a flow over a flat surface.

It can now be derived that the relation

$$\frac{a\,\tau_0}{\eta\,v_0} = -C\ \epsilon_0^{1/2} \tag{18}$$

is universally valid and that constant C only depends on the method of calculation. Therefore a constant C can be calculated both from the exact solution for the flat surface and from (10).

The values for these two constants are given in Table 2. From this table it will be seen that the deviation from $\frac{a\,\tau_0}{\eta\,v_0}$ calculated from (10) is only 8% as compared with the $\frac{a\,\tau_0}{\eta\,v_0}$ which can

(*Continued from page 414*)

INFORMATION RETRIEVAL

Key Words: Pool Boiling-8, Maximum Heat Flux-8, Heat Transfer Coefficient-8, Ethanol Liquid-1, Ethanol Vapor-2, Distilled Water Liquid-1, Steam-2, Capillary Wicking-6, Vapor Venting-6, Acceleration-6, Maximum Heat Flux-7, Heat Transfer Coefficient-7.

Abstract: Boiling heat transfer of ethanol takes place in a pool with the coolant supplied from remote sources by capillary wicking. Heat transfer coefficients are slightly reduced by the capillary material, while the maximum heat flux is adversely affected by the entrapment of vapor in capillary pores. Small accelerations above normal gravity were found to have little effect on maximum heat flux or heat transfer coefficients. With distilled water as a coolant, it is demonstrated that if the vapor produced is properly vented, maximum heat fluxes can be made two or three times as great as those experienced in normal pool boiling. The use of capillary wicking seems promising both in zero gravity and in normal gravity boiling operations.

Reference: Costello, C. P., and E. R. Redeker, **Chem. Eng. Progr. Symposium Ser. No. 41, 59, p. 104 (1963).**

Key Words: Porous Media-5, Heat Transfer-7, Mass Transfer-6, Evaporation-8, Condensation-8, Capillary Flow-8, Diffusion-8, Thermal Conductivity-8, Thermal Diffusivity-8, Drying-8.

Abstract: Measurements were made of the effective thermal conductivities of woven fiber glass sheets wetted with water, benzene, and methanol. When the porous structure is partially saturated with liquid the heat transfer is enhanced by evaporation of liquid in hot regions followed by recondensation in cooler regions. The data were obtained by a dynamic method of recording phase shift and attenuation of a sinusoidal temperature wave as a function of penetration. Results were obtained at temperatures from 25° to 70°C. and at liquid saturations of 0 to 100%.

Reference: Nissan, A. H., David Hansen, and J. L. Walker, **Chem. Eng. Progr. Symposium Ser. No. 41, 59, p. 114 (1963).**

Key Words: Heat Transfer-8, Moving Bed-10, Flat Plate-10, Celite-5, Mica-5, Glass Beads-5, Alumina-5, Vacuum-4, Dichlorodifluoromethane-5, Air-5, Helium-5, Velocity-6, Thermal Diffusivity-6, Length-6, Coefficient-7, Homogeneity-7.

Abstract: Coefficients were measured for a moving bed of fine particles (0.0012 to 0.0150 in.) with various interstitial gases (helium, air, dichlorodifluoromethane) including vacuum. Heat transfer was from electrically heated surfaces (1-1/2, 2-1/4, and 3 in. long) at zero angle of incidence. Velocities of the bed relative to the heat transfer surfaces were varied between 6 to 46 ft./min. The experimental coefficients were compared with the ones predicted from a simple conduction model. The agreement of disagreement between the two depends upon the thermal conductivity of the interstitial fluid, the velocity of the bed, and the length of the heat transfer surface as well as the particle size.

Reference: Harakas, N. K., and K. O. Beatty, Jr., **Chem. Eng. Progr. Symposium Ser. No. 41, 59, p. 122 (1963).**

Key Words: Drying-8, Rotary Dryers-8, Heat Transfer-8, Mass Transfer-8, Differential Equations-10, Wet Pumice-1, Dried Pumice-2, Air Temperature-6, Air Flow-6, Solids Flow-6, Solids Moisture-7, Heat Transfer Coefficient-7, Residence Time-7, Moisture Profiles-7.

Abstract: Heat and mass transfer in rotary dryers were studied theoretically and experimentally. Granular pumice was dried continuously in a perspex dryer, whose efficiency was evaluated by a novel arrangement for temperature measurements. Two methods were used to prepare homogeneously wetted granular material for the tests. Volumetric heat transfer coefficients depended approximately on the 0.8 power of air mass velocity. The dependency of solids residence time on air velocity was also investigated. Determinations of pumice moisture throughout the dryer revealed a maximum deviation of 1% moisture between calculated and measured moisture profiles.

Reference: Myklestad, Ole, **Chem. Eng. Progr. Symposium Ser. No. 41, 59, p. 129 (1963).**

(*Continued on page 416*)

(*Continued from page 415*)

INFORMATION RETRIEVAL

Key Words: A. Moisture Control-8, Rotary Dryers-9, Mathematical Analysis-10, Parameter Adjustments-10, Wet Pumice-1, Dried Pumice-2, Feed Moisture-6, Product Moisture-7. B. Moisture Disturbance-6, Predicted Compensations-7, Control Actions-10, Transient Period-2, Residence Time-7.

Abstract: A mathematical analysis revealed that moisture control in rotary dryers may be carried out by regulation of air temperature, air velocity, and feed rate respectively. Experimental adjustments of these parameters were carried out as compensations for disturbances of the moisture of the raw material (granulated pumice), which was dried continuously. For disturbances as high as 6% moisture, the product could be controlled to within 1% moisture with respect to predicted values. Measurements of process parameters were made during the transient periods subsequent to disturbances and control actions. The transient periods were approximately equal to the residence times under the prevailing conditions.

Reference: Myklestad, Ole, Chem. Eng. Progr. Symposium Ser. No. 41, 59, p. 138 (1963).

Key Words: Transpiration-8, Perforated-5, Tantalum-5, Stainless Steel-5, Dry Nitrogen-5, Ablative-1, Backing-1, Teflon-1, Polystyrene-1, Pyrolyzed-2, Products-2, Heating Rate-6, Application Pressure-6, Degradation Rate-7, Metal Temperature-7.

Abstract: A self-regulating transpiration cooling mechanism is analyzed and investigated experimentally at heating rates up to 1,200 B.t.u./sec. sq. ft. By applying an ablative backing to an electrically heated porous metal surface, a degradation mechanism similar to that associated with the ablation of a reinforced plastic is obtained. The high surface energy absorption characteristic of reinforced plastic degradation is thus retained and the dimensional stability of the cooled surface is also maintained.

Reference: Staub, F. W., and A. E. Flathers, Chem. Eng. Progr. Symposium Ser. No. 41, 59, p. 145 (1963).

Key Words: Heat Transfer-1, *n*-Octadecane-1, Equilibrium-2, Rates-2, Profiles-2, Temperature Gradient-6, Melting-8, Freezing-8, Phase Change-8, Interface-8, Microscope-10, Motion Pictures-10, Anisotropy-, Crystals-.

Abstract: The interface between solid and liquid *n*-octadecane at steady state heat conduction was irregular and in motion when examined by motion picture photography through a microscope. During melting and freezing the interface velocity was definitely faster than predicted by the numerical method of Murray and Landis.

Reference: Thomas, L. J., and J. W. Westwater, Chem. Eng. Progr. Symposium Ser. No. 41, 59, p. 155 (1963).

Key Words: Instrument-8, Enthalpy-6, Measurement-7, Temperature-6, Pressure-6, Gas-1, Dissociation-5, Calorimeter-8, Energy Balance-2, Heat Transfer-2, Cooling-8, Forced Convection-2, Heater-10, Design-8, Fabrication-8, Response-8.

Abstract: An instrument useful for measuring the stagnation enthalpy of a high energy gas stream is described. The instrument operates on a calorimetric basis and the stagnation enthalpy is obtained by an energy balance. The instrument has been evaluated in the temperature range of 1,500° to 4,510° R. and has been shown to operate in a satisfactory manner when compared with other more conventional methods of temperature or energy measurement. Design considerations and an analysis of transient response of the instrument are described.

Reference: Haas, Frederick C., and Franklin A. Vassallo, Chem. Eng. Progr. Symposium Ser. No. 41, 59, p. 165 (1963).

(*Continued on page 417*)

be calculated from the exact solution for the flat surface, so that (7) and (10) describe the flow with reasonable accuracy, also for a large value of ϵ_o.

In approaching the velocity profile according to the Pohlhausen method, the velocity is expressed as a power series in $\frac{y}{\delta}$. When this method is applied to the boundary layer around a cylinder, it appears that this solution does not satisfy the boundary condition on the outside of the boundary layer, whereas for the flat plate it does. In our opinion this drawback has arisen from the change in shape of the viscous part of the boundary layer following the introduction of cylinder coordinates [see (1)].

Transforming the boundary-layer equation by the introduction of new variables in such a way that after the transformation the viscous part of the boundary layer again has the same shape as in the case of the flat surface, compare, for instance, (12), and writing the velocity as a power series in $\hat{\gamma}\left(\hat{\gamma} = \frac{2\gamma}{A}; \frac{A}{2} = \gamma_\delta\right)$ we find that it is possible to satisfy the boundary condition on the outside of the boundary layer. Applying different boundary conditions, we can thus derive different Pohlhausen solutions.

Using the boundary conditions

$$\hat{\gamma} = 0: \quad \alpha = 1, \quad \frac{\partial^2 \alpha}{\partial \gamma^2} = 0;$$

$$\hat{\gamma} = 1: \quad \alpha = 0, \quad \frac{\partial \alpha}{\partial \gamma} = 0$$

we find as solution for the velocity

$$\alpha = 1 - \frac{3}{2}\hat{\gamma} + \frac{1}{2}\hat{\gamma}^3$$

Using the momentum equation, we find for A

$$\frac{72}{A^5}(e^A - 1) - \frac{72}{A^4}e^A + \frac{20}{A^3}\left(e^A + \frac{4}{5}\right) + \frac{1}{A^2}(e^A + 3) + \frac{1}{A}(e^A - 3) - \frac{73}{30} - \sum_{m=1}^{\infty} \frac{A^m}{m.\, m!} = \frac{1}{\epsilon_o} \tag{19}$$

With the boundary conditions

$$\hat{\gamma} = 0: \quad \alpha = 1, \quad \frac{\partial^2 \alpha}{\partial \gamma^2} = 0;$$

$$\hat{\gamma} = 1: \quad \alpha = 0, \quad \frac{\partial \alpha}{\partial \gamma} = 0, \quad \frac{\partial^2 \alpha}{\partial \gamma^2} = 0$$

we find for the velocity

$$\alpha = 1 - 2\hat{\gamma} + 2\hat{\gamma}^3 - \hat{\gamma}^4$$

and A can now be derived from

$$\frac{11520}{A^7}(e^A - 1) - \frac{5640}{A^6}e^A - \frac{5880}{A^6} + \frac{744}{A^5}e^A - \frac{864}{A^5} + \frac{6}{A^4}e^A + \frac{150}{A^4} + \frac{2}{A^3}e^A + \frac{1}{A^2}e^A + \frac{80}{A^3} + \frac{9}{A^2} + \frac{1}{A}e^A + - \frac{4}{A} - \frac{283}{140} - \sum_{m=1}^{\infty} \frac{A^m}{m.\,m!} = \frac{1}{\epsilon_o} \qquad (20)$$

Determining by differentiation from the boundary-layer equation what derivatives become zero on the inside and on the outside of the boundary layer, we obtain the following boundary conditions

$$\hat{\gamma} = 0: \quad \alpha = 1, \quad \frac{\partial^2 \alpha}{\partial \hat{\gamma}^2} = 0;$$

$$\hat{\gamma} = 1: \quad \alpha = 0, \quad \frac{\partial \alpha}{\partial \gamma} = 0, \quad \frac{\partial^2 \alpha}{\partial \gamma^2} = 0, \quad \frac{\partial^3 \alpha}{\partial \gamma^3} = 0$$

and the following velocity

$$\alpha = 1 - \frac{5}{2}\hat{\gamma} + 5\hat{\gamma}^3 - 5\hat{\gamma}^4 + \frac{3}{2}\hat{\gamma}^5$$

A is found from

$$\frac{1814400}{A^9}(e^A - 1) - 589680\frac{e^A}{A^8} - 1224720\frac{1}{A^8} + 51120\frac{e^A}{A^7} - 368640\frac{1}{A^7} + 120\frac{e^A}{A^6} - 58800\frac{1}{A^6} + 24\frac{e^A}{A^5} - 3024\frac{1}{A^5} + 6\frac{e^A}{A^4} + 840\frac{1}{A^4} + 2\frac{e^A}{A^3} + \frac{224}{A^3} + \frac{e^A}{A^2} + \frac{18}{A^2} + \frac{e^A}{A} - \frac{5}{A} - \frac{831}{280} - \sum_{m=1}^{\infty} \frac{A^m}{m.\,m!} = \frac{1}{\epsilon_o} \qquad (21)$$

The solutions (19), (20), and (12)

(*Continued from page 416*)

INFORMATION RETRIEVAL

Key Words: A. Pulsation-6, Heat Transfer-7, Heat Exchanger-10, Siren-10, Sonic-. B. Air-1, Heat Transfer-7. C. Isopropanol-1, Heat Transfer-7, Condensation-7, Condenser-10. D. Air-Isopropanol Mixtures-1, Heat Transfer-7, Dehumidification-7, Cooler Condenser-10.

Abstract: Effects of siren-generated sonic pulsation on heat transfer were studied. Air was cooled, isopropanol vapor was condensed, and air-isopropanol vapor mixtures were dehumidified in a vertical water-cooled tube. Results were interpreted on the basis of a surface-renewal theory.

Reference: Mathewson, W. F., and J. C. Smith, **Chem. Eng. Progr. Symposium Ser. No. 41, 59,** p. 173 (1963).

Key Words: A. Sound-6, Velocity-6, Heat Transfer-7, Mass Transfer-7, Cylinders-10, Naphthalene-10, Air-10, Crossings-, Flow-, Sound-8, Improving-8, Heat Transfer-8, Mass Transfer-8.

Abstract: Heat and mass transfer rates between a cylinder and a cross-flow air stream were increased by imposing an airborne sound of 10 k cycles and 130 decibels on an air flow at $N_{Re} = 80$ to 200. 60 to 90% of this increase could be obtained from entrance effect without a sonic whistle.

Reference: Fussell, Delbert E., and Luh C. Tao, **Chem. Eng. Progr. Symposium Ser. No. 41, 59,** p. 180 (1963).

Key Words: Heat Transfer-, Steam-, Annulus-, Pressure Drop-, Superheated Steam-, Nuclear Superheater-, Experimental Data-, Wet Steam-, Fluid Properties-, Friction Factor.

Abstract: Heat transfer and pressure drop studies have been completed for superheated steam flowing in thin annular passages at 600 lb./sq. in. abs. Local friction factors were measured for both heated and isothermal steam over the complete temperature range. Local heat transfer coefficients were measured on both the inner and outer heat transfer surfaces.

Reference: Neusen, Kenneth F., Glenn J. Kangas, and Neil C. Sher, **Chem. Eng. Progr. Symposium Ser. No. 41, 59,** p. 185 (1963).

Key Words: A. Asymmetric Heating-8, Heat Transfer-8, Convection-8, Kerosene-9, Rockets-10, Hydrocarbon-9, Heat Exchangers-10, Equivalent Diameter-, RP-1-9. B. Electroplating-8, Tubes-9.

Abstract: Forced convection experiments with RP-1 kerosene in a rectangular cross-sectioned passage heated from only a single wall indicate that heat transfer coefficients are lower under conditions of asymmetric heating than with uniform peripheral heating. A unique method of obtaining high asymmetric heat fluxes in an electrically heated apparatus is described. Dimensionless correlation of results is presented graphically.

Reference: Hines, William S., **Chem. Eng. Progr. Symposium Ser. No. 41, 59,** p. 193 (1963).

Key Words: A. Heat Transfer-8, Gas Phase-1, Turbulent Flow-5, Ammonia-1, Helium-1, Experimental-10, Correlations-8, Uniform Heat Flux-10. B. Ammonia-1, Gas Phase-1, Dissociation-6, Molybdenum-4, Stainless Steel-4, High Temperature-10, Low Pressure-10, Round Tube-10, Turbulent Flow-5, Heat Transfer-8.

Abstract: An experimental study of the heat transfer to gaseous ammonia was conducted under conditions of essentially uniform heat flux with fully developed turbulent flow. Both stainless steel and molybdenum test sections heat transfer results were presented as dimensionless correlations. Ammonia dissociation did not appear to influence the heat transfer results; no acoustic resonance was observed. Helium heat transfer results were also obtained.

Reference: McCarthy, J. R., **Chem. Eng. Progr. Symposium Ser. No. 41, 59,** p. 201 (1963).

(*Continued on page 418*)

(*Continued from page 417*)

INFORMATION RETRIEVAL

Key Words: Analysis-, Free Convection-, Heat Transfer-, Boundary Layer-, Dissociation-, Nitrogen Oxides-, Thermal Conductivity-, Specific Heat-, Enthalpy Diffusion-, Temperature Profile-, Velocity Profile-, Nusselt Number-, Prandtl Number-, Grashof Number-, Corrections-, Equilibrium-, Calculations-.

Abstract: A theoretical investigation is made of free convection heat transfer in a dissociating gas enclosed between parallel vertical plates at different temperatures. Numerical calculations are presented for dissociating equilibrium mixtures of nitrogen tetroxide and nitrogen dioxide. Nusselt numbers are given for the overall heat transfer process, and the effect of enclosure geometry upon Nusselt number is explored briefly. The various types of temperature profiles that may be expected in reacting gases are discussed. Numerical results for dissociating nitrogen tetroxide mixtures are compared with correlations based upon frozen transport properties. Calculations are made for the case of a frozen gas layer in chemical equilibrium at the hot and cold plates.

Reference: Scheller, Karl, and Charles E. Dryden, Chem. Eng. Progr. Symposium Ser. No. 41, 59, p. 208 (1963).

approach (18), if $a \to \infty$. For the different solutions different values of C are obtained. These values are given in Table 2.

In the case of the flat plate, Sakiadis (2) found the following relation for the shear stress on the wall

$$\tau_o = -D\,\eta\,v_o \sqrt{\frac{v_o}{\nu x}} \qquad (18)$$

The coefficient D is dependent on the boundary conditions taken into account in deriving the Pohlhausen solution. If we multiply the shear stress on the wall by a, we obtain, by the application of (9),

$$\frac{a\,\tau_o}{\eta\,v_o} = D\sqrt{2}\,\epsilon_o^{1/2}$$

This equation is the same as (18), if

$$C = D\sqrt{2}$$

Now we can calculate C in (18) from the Pohlhausen solutions of the flat plate (Table 2). The C-values of Pohlhausen solution 2 for the flat plate can be obtained from the integral solution of Sakiadis (2) for the flat plate. The other solutions for the flat plate can be obtained in a similar way.

From Table 2 it appears that the C-values for cylindrical surfaces calculated from (19), (20), and (21), and those calculated from the corresponding solutions for the continuous flat surface are identical. The Pohlhausen solutions derived here change for $a \to \infty$ into the Pohlhausen solution for the flat plate. Further we see that the C-value, calculated from the exact solution of the flat plate, is approximated with increasing accuracy as more boundary conditions are used in the Pohlhausen solution.

For large values of ϵ_o the actual boundary layer is described more accurately by the Pohlhausen solutions derived above than by the Sakiadis solution. For small values of ϵ_o the reverse is true. This is remarkable, because in the Pohlhausen solutions the boundary conditions on the outside of the boundary layer are fulfilled for even the value of ϵ_o and in the Sakiadis solution they are only fulfilled for $\epsilon_o = 0$.

The accuracy with which solutions (7) and (10) describe the boundary layer for small values of ϵ_o is clearly demonstrated in Figure 1, where in addition to the theoretical solutions experimental data also have been plotted. These data have been obtained both in measurements of the velocity profile and in direct force measurements on model threads drawn through a water basin.

Table 2. The C-values from (14) Calculated According to Different Methods

<table>
<tr><th>Method</th><th>C calculated from solutions for flat plate</th><th>C calculated from solutions for cylinder</th></tr>
<tr><td>Exact solution</td><td>0.6276</td><td>—</td></tr>
<tr><td>Sakiadis solution*</td><td>—</td><td>0.5774</td></tr>
<tr><td>Pohlhausen solution 1*
Boundary conditions on the outside
$\alpha = 0, \frac{\partial\alpha}{\partial\gamma} = 0$</td><td colspan="2">0.5946</td></tr>
<tr><td>Pohlhausen solution 2*
Boundary conditions on the outside
$\alpha = 0, \frac{\partial\alpha}{\partial\gamma} = 0, \frac{\partial^2\alpha}{\partial\gamma^2} = 0$</td><td colspan="2">0.6053</td></tr>
<tr><td>Pohlhausen solution 3*
Boundary conditions on the outside
$\alpha = 0, \frac{\partial\alpha}{\partial\gamma} = 0, \frac{\partial^2\alpha}{\partial\gamma^2} = 0, \frac{\gamma^3\alpha}{\partial\gamma^3} = 0$</td><td colspan="2">0.6103</td></tr>
</table>

* The boundary conditions on the surface of the cylinder are $\alpha = 1$; $\frac{\partial^2\alpha}{\partial\gamma^2} = 0$.

ACKNOWLEDGMENT

The author wishes to thank the Algemene Kunstzijde Unie for their permission to publish this work.

NOTATION

- x, r = cylindrical coordinates
- u, v = fluid velocity components in the x and r direction
- v_o = cylinder velocity
- a = radius of the cylinder
- η = viscosity
- ν = kinematic viscosity
- δ = boundary-layer thickness
- ϵ_o = dimensionless parameter for the laminar boundary layer
- α, β = dimensionless velocity components
- $\gamma_\delta, \zeta, \gamma, \hat{\xi}, \gamma$ = dimensionless coordinates
- τ_o = shear stress on the wall
- A, B = dimensionless functions of x
- D, C, C_n = dimensionless constants
- K = dimensionless function of a, x, and B

LITERATURE CITED

1. Sakiadis, B. C., *A.I.Ch.E. Journal,* **7,** No. 1, p. 26 (1961).
2. *Ibid.,* No. 2, p. 221.
3. *Ibid.,* No. 3, p. 467.
4. Lighthill, M. J., and M. B. Glauert, *Proc. Rayon Soc. (London),* **230A,** 188. (1955).
5. Jahnke, Emde, and Lösch, *Tafeln höheren Functionen,* Stuttgart (1960).